Experimentally simulating the violation of Bell-type inequalities for generalized GHZ states

Using NMR techniques, we simulate the violations of two Bell-type inequalities: Mermin-Ardehali-Belinskii-Klyshko (MABK) inequality and Chen's inequality[5, 10], for the 3-qubit generalized GHZ states. The experimental results are in good agreement with the quantum predictions and show that Chen's inequality is more efficient than MABK inequality in the case of the generalized GHZ entangled states.

PACS numbers:

Keywords:

I. Introduction

In 1964, Bell showed that in all local realistic theories, correlations between the outcomes of measurements in different parts of a physical system satisfy a certain class of inequalities [1]. However, it is easy to find that entangled states violate these inequalities in quantum mechanics, which shows the crucial conflict between classical theory and quantum mechanics. Hence, Bell's work was described as "the most profound discovery of science" [2] or "one of the greatest discoveries of modern science" [3]. Later, more important generalizations, including the Clauser-Horne-Shimony-Holt (CHSH) [4] and Mermin-Ardehali-Belinskii-Klyshko (MABK) inequalities [5] were developed. Recently, Werner, Wolf, Żukowski and Brukner (WWZB) derived a set of multipartite Bell inequalities, using two dichotomic observables per site [6]. The investigation of Bell's inequalities exhibit fundamental problems of quantum mechanics and also relate to quantum communication [7, 8, 9] and cryptography [10, 11], such as the loophole-free violation of the inequalities is the basis of the security some quantum communication protocols [11, 12]. the inequalities themselves are also useful tools to detect entanglement which is a powerful computational resource in quantum computation [13]. Obviously, further work is worth doing in this domain. Various experiments to test Bell inequality have been performed in various systems including photons [14, 15, 16], atoms systems [17], atomic ensembles [18, 19], and trapped ions [20]. Recently, an experiment to simulate the violation of CHSH inequality was carried out on NMR [21]. All the experiments before were mainly implemented on the maximal entangled states, such as Bell state and the standard GHZ state, but rarely on nonmaximal entangled states, such as the generalized GHZ states. However, many phenomena can only be disclosed by nonmaximal entangled states, for instance, the nonmaximal entangled

states make the maximal violation of many Bell-type inequalities [22, 23]. There are still many open problems about the Bell-type inequalities with nonmaximal entangled states. Therefore, it is interesting and meaningful to study the case of nonmaximal entangled states.

For the three-qubit generalized GHZ states

$$|\Psi\rangle = \cos\theta\,|000\rangle + \sin\theta\,|111\rangle\,, \tag{1}$$

which $\theta \in (0, \frac{\pi}{2})$, Scarani and Gisin [24] firstly found that there existed a region of them satisfying the MABK inequality. It was shown that for $\theta \leq \pi/12$ or $\theta \geq 5\pi/12$ the states (1) do not violate the three-qubit MABK inequality. Later on, Żukowski *et.al* proved that [25] (i) for $N = even$, the generalized GHZ states violate the WWZB inequality, rather than MABK inequalities; (ii) for $N = odd$ and $sin(2\theta) \leq 1/\sqrt{2^{N-1}}$, the generalized GHZ states satisfy both MABK and WWZB inequalities. Soon, Chen and Wu *et al.* developed several Bell inequalities for three qubits, which can be numerically violated by arbitrary generalized GHZ state [26, 27]. Recently, more significant progress was achieved by K. Chen *et al.* [28]. They presented a family of Bell inequalities involving only two measurement settings of each observer for $N > 2$ qubits, which is violated by any N-qubit generalized GHZ state, and moreover the amount of maximal violation grows exponentially as $2^{(N-2)/2}$.

Although there is much theoretical work on nonmaximal entangled states, no experiments aim to display them so far. In this paper, we simulate the violation of two different Bell-type inequalities, i.e., MABK inequality [5] and Chen's inequality [28], for the generalized GHZ states in an NMR system. The experimental results clearly show that the high efficiency of Chen's inequality and the limitation of MABK inequality for any generalized GHZ entangled state and predict the behaviors of quantum mechanics.

II.simulating violation of MABK inequality for GHZ state

Let us consider such a scenario: there are three observers Alice (A), Bob (B), and Charlie (C), each having one qubit. The formulation of the MABK inequality is based on the assumption that every observer is allowed to choose one observable between two dichotomic observables. Denote the outcome of observer X's measurement by $X_i, X = A, B, C$, with $i = 1, 2$. Under the assumption of local realism, each outcome can either take value $+1$ or -1. In a specific run of the experiment, the correlations between the measurement outcomes of all three observers can be represented by the product $A_i B_j C_k$, where $i, j, k = 1, 2$. In a local realistic theory, the correlation function of the

measurements performed by all three observers is the average of $A_iB_jC_k$ over many runs of the experiment,

$$E(A_i, B_j, C_k) =< A_iB_jC_k >_{avg} . \tag{2}$$

The MABK inequality reads as [5]

$$\begin{aligned} | \; & E(A_1, B_2, C_2) + E(A_2, B_1, C_2) + \\ & E(A_2, B_2, C_1) - E(A_1, B_1, C_1)| \leq 2. \end{aligned} \tag{3}$$

We denote the left-hand side of the MABK inequality by $|\mathcal{B}_{MABK}|$ where $-2 \leq \mathcal{B}_{MABK} \leq 2$. In any local hidden variable (LHV) theory, the absolute value of a particular combination of correlations is bounded by 2. However, if one turns to quantum mechanics, this inequality can be violated. For MABK inequality, the maximal violation allowed by quantum mechanics is 4 [24], by the standard GHZ state, i.e., the state with $\theta = \frac{\pi}{4}$ in Eq. (1). As an example, in this section, we simulated the violation of MABK inequality for the standard GHZ state.

To prepare standard GHZ state from $|000\rangle$, we used the network as shown in Fig.1, by selecting the rotation angle $\theta = \pi/4$. After that, we will measure the spin projection $\boldsymbol{\sigma} \cdot \boldsymbol{n}$, where $\boldsymbol{\sigma} = (\sigma_x, \sigma_y, \sigma_z)$ is the vector form of Pauli matrices and the two measurement directions for every qubit we chose here are $\boldsymbol{n_1} = (1, 0, 0)$ and $\boldsymbol{n_2} = (\cos\alpha, \sin\alpha, 0)$. In other words, the two dichotomic observables allowed to be chosen for A,B,C are $\boldsymbol{\sigma}_{\boldsymbol{n_1}}$ and $\boldsymbol{\sigma}_{\boldsymbol{n_2}}$.

For this special spin projection measurement, the theoretical result of $\mathcal{B}_{MABK}$ is (for convenience we just ignore the absolute value sign)

$$\mathcal{B}_{MABK} = 3(\cos^2\alpha - \sin^2\alpha) - 1, \tag{4}$$

demonstrating that for $\alpha = 0.3041\pi \sim 0.6959\pi$, $\mathcal{B}_{MABK} > 2$ it violates MABK inequality and reaches the maximal violation value 4 when $\alpha = \pi/2$.

For NMR experimental implementation, there are still two problems to be solved. Firstly, the thermal equilibrium state of a NMR system at room temperature is highly mixed. We can use pseudo-pure state(PPS) [29] technique to overcome this. Instead of a pure state $|000\rangle$, we prepared a PPS:

$$\rho_{pps} = \frac{(1-\varepsilon)}{2^n} I_{2^n} + \varepsilon \left|000\right\rangle \left\langle 000\right| . \tag{5}$$

It is a mixture of the totally mixed state I_{2^n} unchanged when applying with unitary transformations and a pure state $|000\rangle$ with the polarization $\varepsilon \approx 10^{-5}$. So ignoring I_{2^n} which does not affect NMR experiments and using the entanglement(strictly, pseudo-entanglement) of the pure part, we can simulate violation of the Bell-type inequalities

we mentioned in this letter. The second problem is only the spin projection values under a computational basis can be directly measured. The solution is to rotate the state or density matrix instead of changing the projective direction,

$$M = Tr(\rho \cdot M_1) = Tr(\rho \cdot U^\dagger M_2 U)$$
$$= Tr(U\rho U^\dagger \cdot M_2), \tag{6}$$

where M_1 and M_2 are the desired and experimental measurements, respectively. U is one unitary operation satisfying $M_1 = U^\dagger M_2 U$. In NMR experiments we can apply U to the density matrix and then perform measurement of M_2, which is equivalent to measuring M_1.

All experiments were performed at room temperature on a Bruker Avance 400MHz NMR spectrometer. We used the spins of three ^{13}C nucle in alanine dissolved in D_2O. The system Hamiltonian can be written as

$$H_{sys} = 2\pi \sum_{i=1}^{3} \omega_i I_z^i + 2\pi \sum_{i<j}^{3} J_{ij} I_z^i I_z^j, \tag{7}$$

with the resonance frequencies ω_i and J-coupling constants J_{ij}. The chemical shifts of the three carbon nuclei are $\omega_1 = 5128.2Hz$, $\omega_2 = 17740Hz$, and $\omega_3 = 1676.7Hz$; the J-coupling strengths are $J_{12} = 53.98Hz$, $J_{23} = -1.18Hz$, and $J_{13} = 34.88Hz$.

The whole experiment was divided into three steps. Firstly, to prepare ρ_{pps} from the thermal equilibrium state by using the spatial average technique [30]. Secondly, to prepare a standard GHZ state by using the network in Fig. 1 with $\theta = \pi/4$. Finally, to rotate the required qubits and execute the projective measurements.

In order to improve the accuracy of radio frequency (RF) pulses, we used strongly modulating pulse (SMP) techniques [31]. We also maximized the effective gate fidelity by averaging over a weighted distribution of RF field strengths to overcome the inhomogeneity of the RF fields over the sample. The gate fidelity we calculated for every pulse is higher than 0.995 considering the RF field inhomogeneity. The range of the pulse lengths is approximately from $200 \sim 700\mu s$.

Fig.2 (b) shows a full state tomography of the standard GHZ state prepared in experiment. The overall fidelity is

$$F = \frac{Tr(\rho_{th}\rho_{exp})}{\sqrt{(Tr(\rho_{th}^2)Tr(\rho_{exp}^2))}} = 0.98. \tag{8}$$

We took the observers mentioned above ($\boldsymbol{\sigma_{n_1}}$, $\boldsymbol{\sigma_{n_2}}$) to do the corresponding measurement on the standard GHZ state. The experimental result is shown in Fig.3, where the blue squares stand for the experiment results, and the red thick line stands for the theoretical result. Clearly, the experimental results are in excellent agreement with the theoretical expectation of quantum mechanics.

III. Simulating violation of MABK inequality for generalized GHZ states

So far, almost all previous Bell experiments were performed on maximal entangled states, such as Bell state and the standard GHZ state. Recently, much work about nonmaximal entangled states has been done[22, 23]. In this section, we simulated the violation of MABK inequality for the generalized GHZ state.

In this experiment, we choose the directions of the two measurements for every particle is $\boldsymbol{n_1} = (1, 0, 0)$ and $\boldsymbol{n_2} = (0, 1, 0)$. For these special spin projection measurements, the theoretical result of $\mathcal{B}_{MABK}$ for the generalized GHZ states satisfies such a function,

$$|\mathcal{B}_{MABK}| = |-4\sin(2\theta)|. \tag{9}$$

From Eq. (9), one can see that the maximal violation is obtained when $\theta = \frac{\pi}{4}$ which is just the standard GHZ state. Obviously, the MABK inequality is efficient only in the region of $\theta \in [\frac{\pi}{12}, \frac{5\pi}{12}]$; in other words, only in such a region the inequality can be violated.

We measured a set of generalized GHZ states with particular angles θ. Fig.4(a) shows the experimental date along with the theoretical expectation.

IV. Simulating violation of Chen's inequality for generalized GHZ states

For a three-qubit system, Chen's inequality can be written as

$$\begin{aligned}\mathcal{B}_{Chen} = \frac{1}{2}(&E(A_1, B_1, C_1) + E(A_1, B_2, C_1) + E(A_2, B_1, C_1) - E(A_2, B_2, C_1) + E(A_1, B_1, C_2) + \\ &E(A_1, B_2, C_2) + E(A_2, B_1, C_2) - E(A_2, B_2, C_2)) + E(C_1) - E(C_2),\end{aligned} \tag{10}$$

with $|\mathcal{B}_{Chen}| \leq 2$ in the LHV model.

In the experiment, we took the directions of two measurements about A and B as $\boldsymbol{n_1} = (1, 0, 0)$ and $\boldsymbol{n_2} = (0, 1, 0)$. For C, the directions of two measurement were chosen as $\boldsymbol{n_1} = (\sin\alpha\cos(-\frac{\pi}{4}), \sin\alpha\sin(-\frac{\pi}{4}), \cos\alpha)$ and $\boldsymbol{n_2} = (\sin(\pi-\alpha)\cos(-\frac{\pi}{4}), \sin(\pi-\alpha)\sin(-\frac{\pi}{4}), \cos(\pi-\alpha))$, where

$$\begin{aligned}\alpha &= \tan^{-1}[\sqrt{2}\tan(2\theta)], \qquad 0 \leq \theta \leq \frac{\pi}{4} \\ \alpha &= \tan^{-1}[\sqrt{2}\tan(2\theta)] + \pi, \qquad \frac{\pi}{4} \leq \theta \leq \frac{\pi}{2}\end{aligned} \tag{11}$$

Then, we obtain $\mathcal{B}_{Chen}$ as

$$\mathcal{B}_{Chen} = 2[2\sin^2(2\theta) + \cos^2(2\theta)]^{1/2}, \tag{12}$$

which tells us that $\mathcal{B}_{Chen}$ is always larger than 2 no matter whatever θ is. It illustrates that the whole region of the generalized GHZ states can violate the inequality by a set of suitable observation angles.

Obviously, Chen's inequality is more efficient than MABK inequality for generalized GHZ states. The experimental result is shown in Fig.4(b), which perfectly simulates the violation of Chen's inequality for the generalize GHZ states.

V. Conclusions

In summary, we have investigated the simulation of the violation of Bell-type inequalities, including MABK inequality and Chen's inequality for the generalized GHZ states in an NMR system. In the range of the generalized GHZ states, Chen's inequality is more efficient than MABK inequality. The experimental results are well in agreement with the theoretical expectation.

It is necessary to emphasize that, in strict, because NMR qubits are many nuclear spins of atoms bounded together in a single molecule, separated by a few angstroms, the NMR experiment is inherently local. However, the meaning is that, when we experimentally simulate the violation of different Bell-type inequalities for arbitrarily generalized three-qubit GHZ states in NMR, the results are excellently in according with the quantum predictions. Despite of many existing disputes, NMR may contribute more on some fundamentals of quantum mechanics. As a refined tool and technique for experimentally realizing quantum computation in the last decade, NMR is still helpful in solving numerous fundamental problems of quantum mechanics now.

[1] J. S. Bell, Physics (Long Island city, N.Y) **1**,195 (1964).

[2] H. P. Stapp, Nuovo Cimento Soc. Ital. Fis. B **29**, 270 (1975).

[3] M. Żukowski, Stud. Hist. Phil. Mod. Phys. **36**, 566 (2005).

[4] J. Clauser, M. Horne, A. Shimony, and R. Holt, Phys. Rev. Lett. **23**, 880 (1969).

[5] N. D. Mermin, Phys. Rev. Lett. **65**, 1838 (1990); S. M. Roy and V. Singh, ibid. **67**, 2761 (1991); M. Ardehali, Phys. Rev. A **46**, 5375 (1992); A. V. Belinskii and D. N. Klyshko, Phys. Usp. **36**, 653 (1993); N. Gisin and H. Bechmann-Pasquinucci, Phys. Lett. A **246**, 1 (1998).

[6] R. F. Werner and M. M. Wolf, Phys. Rev. A **64**, 032112 (2001); M. Żukowski and Č Brukner, Phys. Rev. Lett. **88**, 210401 (2002).

[7] Č Brukner, M. Żukowski, J. W Pan, and A. Zeilinger, Phys. Rev. Lett. **92**, 127901 (2004).

[8] G. Brassard, H. Buhrman, N. Linden, A. A. Méthot, A. Tapp, and F. Unger, Phys. Rev. Lett. **96**, 250401 (2006).

[9] V. Scarani, and N. Gisin, Phys. Rev. Lett. **87**, 117901 (2001).

[10] Z. B. Chen, Q. Zhang, X. H Bao, J. Schmiedmayer and J. W. Pan, Phys. Rev. A **73**, 050302(R) (2006).

[11] A. Acín, N. Gisin, and L. Masanes, Phys. Rev. Lett. **97**, 120405 (2006).

[12] A. Acín, N. Brunner, N. Gisin, S. Massar, S. Pironio, V. Scarani, Phys. Rev. Lett. **98**, 230501 (2007).

[13] M. A. Nielsen, and I. L. Chuang, Quantum Computation and Quantum Information (Cambridge: Cambridge University Press) (2000).

[14] S. J. Freedman and J. F. Clauser, Phys. Rev. Lett. **28**, 938 (1972).

[15] A. Aspect, J. Dalibard, and G. Roger, Phys. Rev. Lett. **49**, 1804 (1982).

[16] G. Weihs, T. Jennewein, C. Simon, H. Weinfurter, and A. Zeilinger, Phys. Rev. Lett. **81**, 5039 (1998).

[17] D. L. Moehring, M. J. Madsen, B. B. Blinov, and C. Monroe, Phys. Rev. Lett. **93**, 090410 (2004).

[18] D. N. Matsukevich et al., Phys. Rev. Lett. **96**, 030405 (2006).

[19] C.-W. Chou et al., Science **316**, 1316 (2007).

[20] M. A. Rowe et al., Nature (London) **409**, 791 (2001).

[21] A. M. Souza et al., New. J. Phys. **10**, 033020 (2008).

[22] A. Acín,, T. Durt, N. Gisin and J. I. Latorre, Phys. Rev. A **65**, 052325 (2002).

[23] A. A. Méthot and V. Scarani, Quant. Inf. Comput. **7**, 157 (2007).

[24] V. Scarani and N. Gisin, J. Phys. A **34**, 6043 (2001).

[25] M. Żukowski, Č Brukner, W. Laskowski, and M. Wiesniak, Phys. Rev. Lett. **88**, 210402 (2002).

[26] J. L. Chen, C. F. Wu, L. C. Kwek, and C. H. Oh, Phys. Rev. Lett. **93**, 140407 (2004).

[27] C. F. Wu, J. L. Chen, L. C. Kwek, and C. H. Oh, Phys. Rev. A **77**, 062309 (2008).

[28] K. Chen, S. Albeverio, and S. M. Fei, Phys. Rev. A **74**, 050101(R)(2006).

[29] N. A. Gershenfeld, I. L. Chuang, Science **275**, 350-356 (1997).

[30] D. G. Cory, A. F. Fahmy and T. F. Havel, Proc. Natl. Acad, Sci. USA, **94**, 1634 (1997).

[31] E. Fortunato *et al.*, Chem. Phys. **116**(17), 7599 (2002).

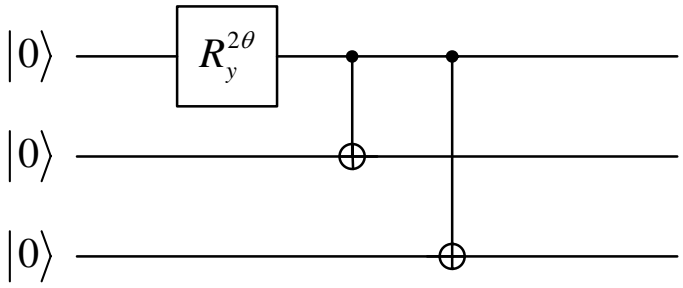

FIG. 1: Quantum network for creating a generalized GHZ state. The input state is $|000\rangle$. $R_y^{2\theta}$ denotes a rotation of an angle 2θ along Y axis, following by two controlled-not (CNOT) gates. The output state is a generalized GHZ state $\cos\theta\,|000\rangle + \sin\theta\,|111\rangle$.

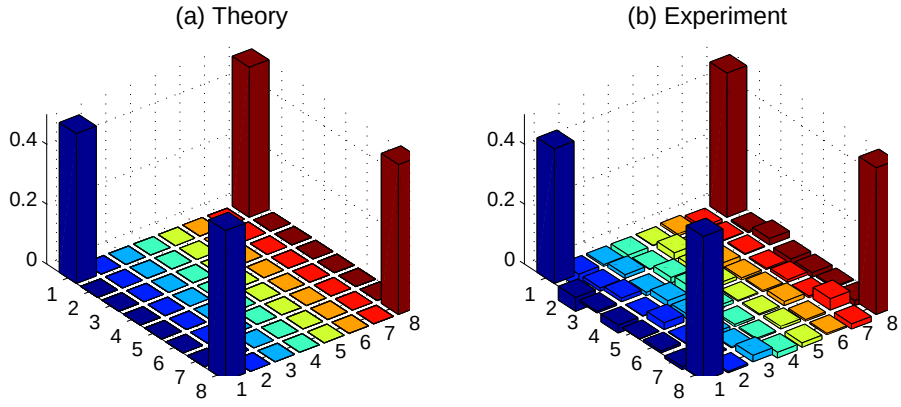

FIG. 2: Theoretical (a) and experimental (b) density matrices of the standard GHZ state $(|000\rangle + |111\rangle)/\sqrt{2}$.

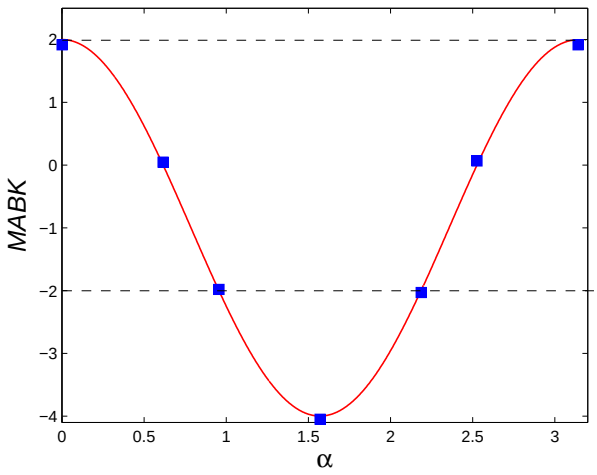

FIG. 3: Experimental test of the MABK inequality for a standard GHZ state. The red thick line stands for the theoretical expectation, and the blue square stands for the experimental data.

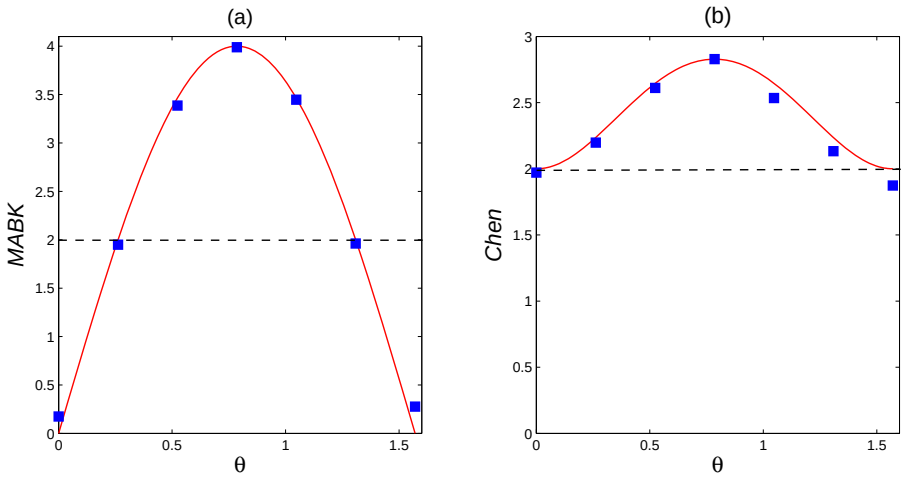

FIG. 4: For the generalized GHZ states, (a) the values of $\mathcal{B}_{MABK}$ as a function of θ, (b) the values of $\mathcal{B}_{Chen}$ as a function of θ. The red thick line stands for the theoretical expectation, and the blue square stands for the experiment data.